



DALHOUSIE UNIVERSITY

Retrieved from DalSpace, the institutional repository of
Dalhousie University

<https://dalspace.library.dal.ca/handle/10222/79575>

Version: Post-print

Publisher's version: Feng, Xibo, Becke, Axel, Johnson, Erin.
(2018). Becke's virial exciton model gives accurate charge-
transfer excitation energies. *J. Chem. Phys.* 149, 231101 (2018).
doi.org/10.1063/1.5078515

Becke's Virial Exciton Model Gives Accurate Charge-Transfer Excitation Energies

Xibo Feng,¹ Axel D. Becke,¹ and Erin R. Johnson^{1, a)}

Department of Chemistry, Dalhousie University, 6274 Coburg Rd, P.O. Box 15000, Halifax, Nova Scotia, B3H 4R2, Canada

(Dated: 24 November 2018)

First singlet (S_1) excitations are of primary importance in the photoluminescence spectra of organic chromophores. However, due to the multi-determinantal nature of the singlet excited states, standard Kohn-Sham density-functional theory (DFT) is not applicable. While linear-response time-dependent DFT is the method of choice for the computation of excitation energies, it fails severely for excitations with charge-transfer character. Becke's recent virial exciton model [J. Chem. Phys. **148**, 044112 (2018)] offers a promising solution to employ standard DFT for calculation of the S_1 excitation energy in molecular systems. Here, it is shown that the virial exciton model is free of charge-transfer error. It is equally reliable for S_1 excitations with significant charge-transfer character as for other classes of transitions.

^{a)}Electronic mail: erin.johnson@dal.ca

I. INTRODUCTION

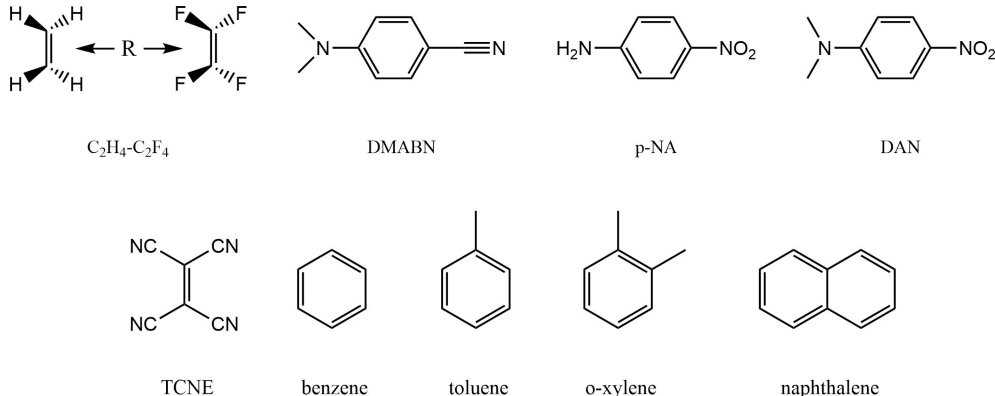
The photoluminescence of organic chromophores plays a fundamental role in nature, with prominent examples being photosynthesis,¹ vision,² and bioluminescence³. Recent applications of photoluminescent materials include development of organic light-emitting diodes,^{4,5} fluorescent sensors,^{6,7} lasers,⁸ waveguides,⁹ and biomedical imaging.^{7,10} The first singlet (S_1) electronic excitation is of primary importance in photoluminescence spectra. Computational modeling of these excitations is complicated as standard Kohn-Sham density-functional theory (DFT)¹¹ is not applicable to the S_1 excited state due to its multi-determinant nature. Linear-response time-dependent density-functional theory (TD-DFT)¹²⁻¹⁴ is the predominant method employed for the calculation of S_1 , and higher, excitation energies. However, TD-DFT typically exhibits a severe underestimation of the excitation energy (frequently in excess of 1 eV) when the excitation is of charge-transfer (CT) character¹⁵⁻¹⁹. This problem can be ameliorated using long-range-corrected hybrid functionals, but the optimum range-separation parameter in these functionals is extremely system dependent.²⁰⁻²² Also, time-independent methods as exemplified by the very recent work of the Van Voorhis group (see Ref. 23 and references therein) are known which can handle CT excitations well. We recommend Ref. 24 for extensive reviews of both time-dependent and time-independent approaches to excited states in DFT.

Becke recently derived a simple model²⁵ for the energy splitting between the first singlet and triplet (S_1 - T_1) excited states, and hence the S_1 excitation energy itself, based on the virial theorem.²⁶ This “virial exciton model” only requires conventional DFT calculations for the S_0 ground state and the (single-determinant) T_1 excited state. It therefore represents a simple alternative to TD-DFT for calculation of the S_1 excitation energy in molecular systems. For Thiel’s benchmark set²⁷ of 28 small-molecule excitation energies, the virial exciton model achieves a mean absolute error (MAE) for S_1 on par with TD-B3LYP (0.26 and 0.24 eV, respectively), relative to high-level correlated wavefunction reference data. Remarkably, it significantly out-performs TD-B3LYP for S_1 excitation energies of polycyclic aromatic hydrocarbons,²⁸ achieving a MAE of 0.13 eV, versus the TD-B3LYP value of 0.31 eV.²⁵

In this work, the performance of the virial exciton model for systems that feature S_1 excitations of significant CT character will be assessed for the first time. It is a two-step

method, beginning with a conventional T_1 excitation-energy computation, followed by a simple two-electron integral correction. The first step ensures, in large part, that the method does not suffer the CT failures of TD-DFT. Our benchmark set (see Fig. 1) consists of three subsets: (i) the ethylene-tetrafluoroethylene intermolecular CT dimer that has been used as a classic demonstration of TD-DFT charge-transfer error;¹⁶ (ii) four intermolecular CT dimers consisting of tetrafluoroethylene and aromatic hydrocarbons, for which experimental S_1 excitation energies are available;^{29,30} and (iii) three donor-acceptor molecules featuring S_1 excitations with intramolecular CT, for which high-level correlated wavefunction benchmark data are available.^{31,32} The results show that the virial exciton model is free of CT error.

FIG. 1: The chemical systems investigated in this work. Shown are the ethylene-tetrafluoroethylene ($C_2H_4-C_2F_4$) complex; the donor-acceptor molecules 4-dimethylamino-benzonitrile (DMABN), *para*-nitroaniline (p-NA), and *N,N*-dimethyl-4-nitroaniline (DAN); and the intermolecular CT dimers between tetracyanoethylene (TCNE) and each of benzene, toluene, *o*-xylene, and naphthalene.



II. THEORY

In the virial exciton model, the difference between the S_1 and T_1 excitation energies is given by the following two-electron integral:

$$\Delta E_{ST} = K_{if} = \int \int d^3\mathbf{r}_1 d^3\mathbf{r}_2 \frac{\phi_i(\mathbf{r}_1)\phi_f(\mathbf{r}_1)\phi_i(\mathbf{r}_2)\phi_f(\mathbf{r}_2)}{r_{12}}, \quad (1)$$

where ϕ_i and ϕ_f are the initial and final Kohn-Sham (KS) orbitals involved in the single-electron excitation, respectively. This expression is the result of adding a correlation cor-

rection to the uncorrelated S₁-T₁ splitting. In the following, we briefly summarise how this result is derived.

For a non-interacting system, the S₁-T₁ excitation-energy difference is

$$\Delta E_{\text{ST}}^0 = \frac{1}{2} \int \int d^3\mathbf{r}_1 d^3\mathbf{r}_2 \frac{\Delta \Pi_{\text{ST}}^0(\mathbf{r}_1, \mathbf{r}_2)}{r_{12}}, \quad (2)$$

where $\Delta \Pi_{\text{ST}}^0(\mathbf{r}_1, \mathbf{r}_2)$ is the non-interacting pair-density difference between the S₁ and T₁ states:

$$\Delta \Pi_{\text{ST}}^0(\mathbf{r}_1, \mathbf{r}_2) = 4\phi_i(\mathbf{r}_1)\phi_f(\mathbf{r}_1)\phi_i(\mathbf{r}_2)\phi_f(\mathbf{r}_2). \quad (3)$$

Substituting eq. 3 into eq. 2, one obtains

$$\Delta E_{\text{ST}}^0 = 2 \int \int d^3\mathbf{r}_1 d^3\mathbf{r}_2 \frac{\phi_i(\mathbf{r}_1)\phi_f(\mathbf{r}_1)\phi_i(\mathbf{r}_2)\phi_f(\mathbf{r}_2)}{r_{12}} = 2K_{if}. \quad (4)$$

A correlation correction, $\Delta E_{\text{ST}}^{\text{corr}}$, must be added to ΔE_{ST}^0 to recover the correlated S₁-T₁ splitting, ΔE_{ST} :

$$\Delta E_{\text{ST}} = \Delta E_{\text{ST}}^0 + \Delta E_{\text{ST}}^{\text{corr}}. \quad (5)$$

$\Delta E_{\text{ST}}^{\text{corr}}$ consists of kinetic and potential energy contributions:

$$\Delta E_{\text{ST}}^{\text{corr}} = \Delta T_{\text{ST}}^{\text{corr}} + \Delta V_{\text{ST}}^{\text{corr}}. \quad (6)$$

The quantum virial theorem states that, for a system at equilibrium, its kinetic (T) and potential (V) energies have the simple relation $2T = -V$. This theorem is valid for both the ground and excited states. It also equally applies to both the correlated and uncorrelated systems. Therefore, this theorem can be used to simplify eq. 6 and write

$$\Delta E_{\text{ST}}^{\text{corr}} = \frac{1}{2} \Delta V_{\text{ST}}^{\text{corr}}. \quad (7)$$

Becke argued²⁵ that electron correlation would have the effect of “smoothing out” the S₁-T₁ non-interacting pair-density difference (eq. 3), reducing it to zero everywhere. Correlation would then lower the potential energy of the S₁ state, relative to the T₁ state, by $\Delta V_{\text{ST}}^{\text{corr}} = -2K_{if}$. Thus,

$$\Delta E_{\text{ST}}^{\text{corr}} = -K_{if} \quad (8)$$

and substitution into eq. 5 gives the correlated S₁-T₁ splitting,

$$\Delta E_{\text{ST}} = 2K_{if} - K_{if} = K_{if}, \quad (9)$$

which is the result in eq. 1.

The S_1 energy, E_{S_1} , and the corresponding excitation energy, $\Delta E_{0S} = E_{S_1} - E_{S_0}$, can therefore be obtained from the energies of the S_0 and T_1 states and the K_{if} integral by

$$E_{S_1} = E_{T_1} + K_{if}, \quad (10a)$$

$$\Delta E_{0S} = E_{T_1} + K_{if} - E_{S_0} = E_{0T} + K_{if}, \quad (10b)$$

where $\Delta E_{0T} = E_{T_1} - E_{S_0}$ is the triplet excitation energy. To evaluate ΔE_{0S} , the virial exciton model requires the energy of the S_0 state, as well as a restricted-open-shell (RO) calculation for the T_1 state. The calculation must be RO in order to uniquely define ψ_i and ψ_f .

III. COMPUTATIONAL DETAILS

The geometries of the four TCNE-aromatic dimers (B3LYP/cc-pVDZ),²⁹ and DMABN (B3LYP/6-31G*)³² were taken from the literature. The geometries of p-NA and DAN were optimized using B3LYP/6-311G(d,p), consistent with Ref. 31. The $C_2H_4-C_2F_4$ dimer geometry (C_{2v} symmetry) was optimized using B3LYP/6-31+G* at a fixed intermolecular separation of 4 Å. This intermolecular separation, R , was defined by the distance between the midpoints of the two C=C bonds, as shown in Figure 1, and was varied from 4.0 to 10.0 Å in 0.5 Å increments. Ground-state, unrestricted and RO triplet-state, and TD-DFT single-point calculations, were performed on the optimized geometries of all species using B3LYP^{33,34}/cc-pVTZ. Configuration interaction singles (CIS)³⁵ calculations were also performed using the cc-pVTZ basis set for the $C_2H_4-C_2F_4$ dimer. The Gaussian 09 package³⁶ was employed throughout. An in-house “postG” program was used to compute the K_{if} integrals employing the numerical method of Becke and Dickson.³⁷

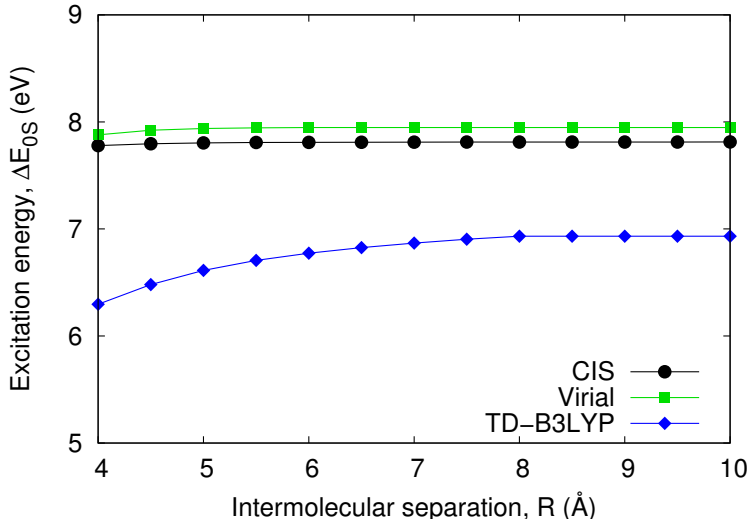
IV. RESULTS AND DISCUSSION

A. $C_2H_4-C_2F_4$: A Classic CT Test

We first apply the virial exciton model to the $C_2H_4-C_2F_4$ intermolecular dimer,¹⁶ which is an established test of CT-excitation errors. The S_1 excitation energy was calculated for

a range of intermolecular separations with the virial exciton model, TD-B3LYP, and CIS. The results are shown in Figure 2.

FIG. 2: Calculated S_1 excitation energy (E_{0S}) as a function of the intermolecular separation, R , for the $C_2H_4-C_2F_4$ dimer. The B3LYP functional was used for both the TD-DFT and virial exciton model calculations.



CIS theory, which will serve as our benchmark, predicts a localized $\pi \rightarrow \pi^*$ transition on the ethylene molecule as the lowest-energy singlet excitation. In contrast, various TD-DFT calculations erroneously predict the intermolecular CT state to lie lower in energy.^{16,38} This causes TD-B3LYP to drastically underestimate the S_1 excitation energy over the entire range of intermolecular separations. Moreover, because the TD-B3LYP S_1 excitation has CT character, the excitation energy shows a strong dependence on the intermolecular distance, as seen in Figure 2. Conversely, the lowest-energy triplet excitation is localized on the ethylene molecule and is of $\pi \rightarrow \pi^*$ character. As a result, the virial exciton model is in good agreement with CIS over the entire range of intermolecular separations and does not share the same CT breakdown displayed by TD-B3LYP.

Calculations were also attempted on the bacteriochlorin-zincbacteriochlorin intermolecular dimer, which is a second complex popularized as a demonstration of CT error.³⁸ However, due to the near degeneracy of the first three excited states³⁸, we have not yet been able to converge the RO triplet calculations required for the virial exciton model.

B. TCNE-Aromatic Dimers and Push-Pull Dye Molecules

We now turn to a set of systems for which the S_1 excitation does correspond to a CT state. The S_1 excitation energies were computed for four TCNE-aromatic CT dimers and three donor-acceptor molecules featuring intramolecular CT excitations. The resulting excitation energies, and related quantities required for the virial exciton model, are tabulated in Table 1. The S_1 excitation energies are compared to experimental or high-level theoretical reference values.^{29,31,32}

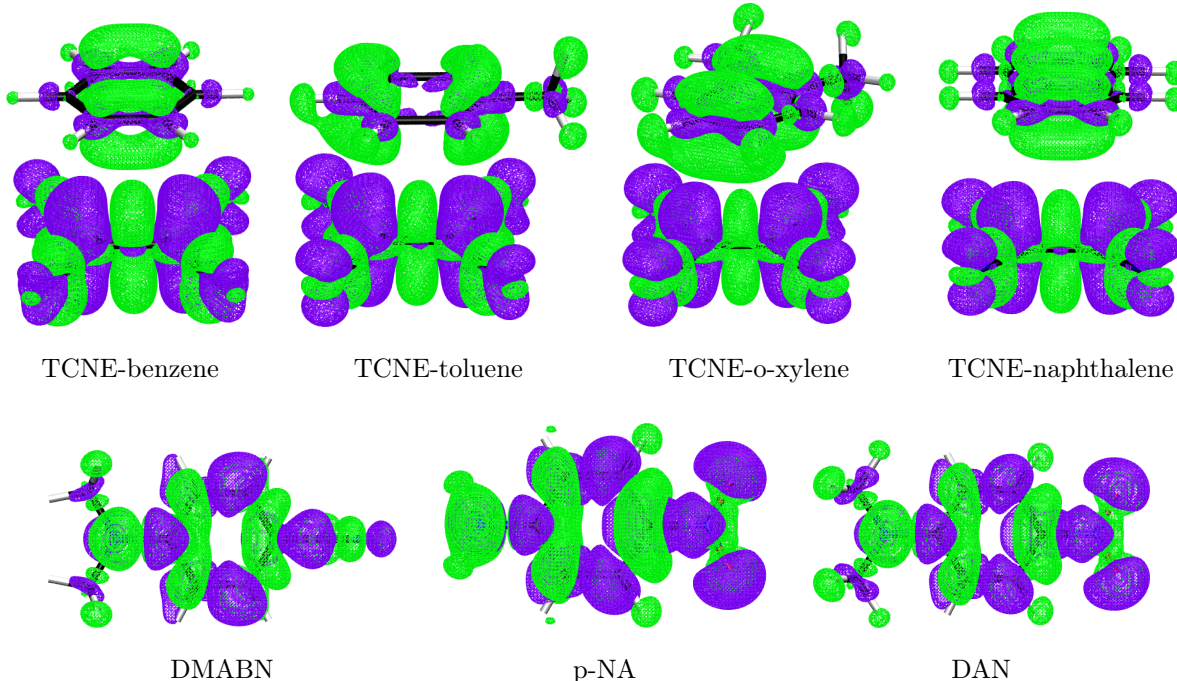
TABLE I: Calculated excitation energies, and related quantities, in eV. Absolute errors from the literature reference values ($\Delta E_{0S}^{\text{Ref.}}$) are given in parentheses. Tabulated values are: the unrestricted and restricted T_1 excitation energies (ΔE_{0T}^U and $\Delta E_{0T}^{\text{RO}}$), the K_{if} integral, the unrestricted and restricted S_1 excitation energies (ΔE_{0S}^U and $\Delta E_{0S}^{\text{RO}}$), and the TD-B3LYP S_1 excitation energies ($\Delta E_{0S}^{\text{TD}}$).

System	ΔE_{0T}^U	$\Delta E_{0T}^{\text{RO}}$	K_{if}	ΔE_{0S}^U	$\Delta E_{0S}^{\text{RO}}$	$\Delta E_{0S}^{\text{TD}}$	$\Delta E_{0S}^{\text{Ref.}}$
TCNE-benzene	2.27	2.41	1.55	3.82 (0.23)	3.96 (0.37)	1.91 (-1.68)	3.59 ²⁹
TCNE-toluene	2.21	2.33	1.30	3.51 (0.15)	3.63 (0.27)	1.74 (-1.62)	3.36 ²⁹
TCNE-o-xylene	2.14	2.25	1.12	3.26 (0.11)	3.37 (0.22)	1.48 (-1.67)	3.15 ²⁹
TCNE-naphthalene	1.61	1.72	1.10	2.71 (0.11)	2.82 (0.22)	0.81 (-1.79)	2.60 ²⁹
DMABN	3.33	3.41	1.66	4.99 (0.27)	5.07 (0.35)	4.31 (-0.41)	4.72 ³²
p-NA	3.12	3.17	1.46	4.58 (0.19)	4.63 (0.24)	3.50 (-0.89)	4.39 ³¹
DAN	2.91	2.97	1.37	4.28 (0.34)	4.34 (0.40)	3.19 (-0.75)	3.94 ³¹
MAE				0.20	0.29	1.26	–

To verify that the T_1 excited states in question indeed possess CT character, we computed density differences relative to the S_0 ground state. The results are presented in Figure 3. For each of the four TCNE-aromatics dimers, notable intermolecular CT is observed, with the electron density shifting from the aromatic moiety to the TCNE molecule. DMABN, p-NA, and DAN all show typical intramolecular, push-pull CT from the electron-donating to the electron-withdrawing substituent.

Returning to Table I, the S_1 - T_1 energy splitting, given by the K_{if} integral, ranges from

FIG. 3: Computed T_1 - S_0 density differences for the TCNE-aromatic dimers and donor-acceptor molecules. Violet (green) isosurfaces represent an increase (decrease) in electron density in the T_1 state relative to the S_0 state. The isovalues are ± 0.001 a.u.



1.1-1.7 eV for these systems. One might expect a vanishing K_{if} integral for CT excitations, as the ground-state frontier orbitals will be localised on either the donor or acceptor moieties and will consequently have negligible overlap. However, this is not the case, as the two singly-occupied molecular orbitals in the RO triplet calculations are delocalised over both moieties and have substantial overlap.

Table I shows that TD-B3LYP drastically underestimates the CT excitation energies, as expected, with a MAE of 1.26 eV. For all seven systems, the virial exciton model provides significantly more accurate CT excitation energies than TD-B3LYP, with a MAE of 0.29 eV. An even lower MAE of 0.20 eV can be achieved by adding K_{if} (which must be computed from the RO triplet orbitals) to the *unrestricted* T_1 excitation energy. Contrary to the typical underestimation by TD-DFT methods, the virial exciton model systematically overestimates the CT excitation energies in Table I. This is possibly a result of using the cc-pVTZ basis set, which lacks diffuse functions. The CT nature of the present excitations results in anionic moieties in the excited states, which will be preferentially stabilised by the addition of diffuse

functions. Unfortunately, the RO triplet calculations are somewhat difficult to converge with the present basis set, and addition of diffuse functions greatly exacerbates the problem. This emphasizes the importance of improving self-consistent-field algorithms for RO calculations, as one must be able to efficiently converge to the correct triplet state before applying the virial correction. Regardless, the performance of the virial exciton model is impressive and confirms that it does not suffer from the same intrinsic CT errors as TD-DFT.

V. CONCLUSIONS

In this work, the accuracy of Becke’s virial exciton model was assessed for CT excitation energies. The results demonstrate that the model is free of the systematic CT errors that plague conventional TD-DFT methods. For a benchmark set consisting of four intermolecular TCNE-aromatic dimers and three donor-acceptor molecules, the virial exciton model achieves an overall MAE of 0.29 eV (or 0.20 eV using unrestricted T_1 energies) compared to literature reference data, significantly improving upon the accuracy of the widely used TD-B3LYP method. This error is roughly on par with the MAE of 0.26 eV previously obtained²⁵ for Thiel’s small-molecule excitation data set.²⁷ We therefore conclude that the virial exciton model can be reliably used to predict S_1 excitation energies in molecular systems, even for excitations with CT-character. See, also, the very recent application of the model to computation of the optical gap in polyacetylene.³⁹

VI. ACKNOWLEDGEMENTS

E.R.J. and A.D.B. thank the Natural Sciences and Engineering Research Council of Canada (NSERC), and F. X. acknowledges the Government of Nova Scotia, for financial support. Computational resources were provided by ACEnet, the Atlantic Computational Excellence Network, funded by Compute Canada.

REFERENCES

¹N. Murata, *Biochim. Biophys. Acta* **172**, 242 (1969).

²K. Palczewski, *J. Biol. Chem.* **287**, 1612 (2012).

- ³I. Navizet, Y.-J. Liu, N. Ferré, D. Roca-Sanjuán, and R. Lindh, *ChemPhysChem* **12**, 3064 (2011).
- ⁴H. Sasabe and J. Kido, *Eur. J. Org. Chem.* **34**, 7653 (2013).
- ⁵H. Kaji, C. Adachi, *et al.*, *Nat. Commun.* **6**, 8476 (2015).
- ⁶X. Hou, C. Ke, C. J. Bruns, P. R. McGonigal, R. B. Pettman, and J. F. Stoddart, *Nat. Commun.* **6**, 6884 (2015).
- ⁷L.-L. Li, K. Li, Y.-H. Liu, H.-R. Xu, and X.-Q. Yu, *Sci. Rep.* **6**, 31217 (2016).
- ⁸S. Chénais and Forget, *Polym. Int.* **61**, 390 (2012).
- ⁹Y. Jiang, Z. Da, F. Qiu, Y. Guan, and G. Cao, *J. Nonlinear Opt. Phys. Mater.* **26**, 1750032 (2017).
- ¹⁰K. Kundu, S. Knight, N. Willett, S. Lee, W. Taylor, and N. Murthy, *Angew. Chem. Int. Ed.* **48**, 299 (2009).
- ¹¹W. Kohn and L. J. Sham, *Phys. Rev.* **140**, A 1133 (1965).
- ¹²E. Runge and E. K. U. Gross, *Phys. Rev. Lett.* **52**, 997 (1984).
- ¹³M. Petersilka, U. J. Gossmann, and E. K. U. Gross, *Phys. Rev. Lett.* **76**, 1212 (1996).
- ¹⁴R. Bauernschmitt and R. Ahlrichs, *Chem. Phys. Lett.* **265**, 454 (1996).
- ¹⁵D. J. Tozer, *J. Chem. Phys.* **119**, 12697 (2003).
- ¹⁶A. Dreuw, J. L. Weisman, and M. Head-Gordon, *J. Chem. Phys.* **119**, 2943 (2003).
- ¹⁷O. Gritsenko and E. J. Baerends, *J. Chem. Phys.* **121**, 655 (2004).
- ¹⁸M. J. G. Peach, P. Benfield, T. Helgaker, and D. J. Tozer, *J. Chem. Phys.* **128**, 044118 (2008).
- ¹⁹M. E. Casida, *J. Mol. Struct. (Theochem)* **914**, 3 (2009).
- ²⁰T. Koerzdoerfer, J. S. Sears, C. Sutton, and J. L. Bredas, *J. Chem. Phys.* **135**, 204107 (2011).
- ²¹L. Kronik, T. Stein, S. Refaely-Abramson, and R. Baer, *J. Chem. Theory Comput.* **8**, 1515 (2012).
- ²²K. Garrett, X. A. Sosa Vazquez, S. B. Egri, J. Wilmer, L. E. Johnson, B. H. Robinson, and C. M. Isborn, *J. Chem. Theory Comput.* **10**, 3821 (2014).
- ²³D. Hait, T. Zhu, D. P. McMahon, and T. Van Voorhis, *J. Chem. Theory Comput.* **12**, 3353 (2016).
- ²⁴N. Ferré, M. Filatov, and M. Huix-Rotllant, eds., *Topics in Current Chemistry*, Vol. 368 (Springer International Publishing, Switzerland, 2016).

- ²⁵A. D. Becke, *J. Chem. Phys.* **148**, 044112 (2018).
- ²⁶I. N. Levine, *Quantum Chemistry, 7th ed.* (Pearson Education, Inc., Upper Saddle River, NJ, USA, 2014).
- ²⁷M. R. Silva-Junior, M. Schreiber, S. P. A. Sauer, and W. Thiel, *J. Chem. Phys.* **133**, 174318 (2010).
- ²⁸M. Parac and S. Grimme, *Chem. Phys.* **292**, 11 (2003).
- ²⁹T. Stein, L. Kronik, and R. Baer, *J. Am. Chem. Soc.* **131**, 2818 (2009).
- ³⁰I. Hanazaki, *J. Phys. Chem.* **76**, 1982 (1972).
- ³¹H. Sun and J. Autschbach, *ChemPhysChem* **14**, 2450 (2013).
- ³²M. Barry, II, H. Sun, N. Govind, K. Kowalski, and J. Autschbach, *J. Chem. Theory Comput.* **11**, 3305 (2015).
- ³³A. D. Becke, *J. Chem. Phys.* **98**, 5648 (1993).
- ³⁴P. J. Stephens, F. J. Devlin, C. F. Chabalowski, and M. J. Frisch, *J. Phys. Chem.* **98**, 11623 (1994).
- ³⁵J. B. Foresman, M. Head-Gordon, J. A. Pople, and M. J. Frisch, *J. Phys. Chem.* **96**, 135 (1992).
- ³⁶M. J. Frisch, G. W. Trucks, H. B. Schlegel, G. E. Scuseria, M. A. Robb, J. R. Cheeseman, G. Scalmani, V. Barone, B. Mennucci, G. A. Petersson, H. Nakatsuji, M. Caricato, X. Li, H. P. Hratchian, A. F. Izmaylov, J. Bloino, G. Zheng, J. L. Sonnenberg, M. Hada, M. Ehara, K. Toyota, R. Fukuda, J. Hasegawa, M. Ishida, T. Nakajima, Y. Honda, O. Kitao, H. Nakai, T. Vreven, J. A. Montgomery, Jr., J. E. Peralta, F. Ogliaro, M. Bearpark, J. J. Heyd, E. Brothers, K. N. Kudin, V. N. Staroverov, R. Kobayashi, J. Normand, K. Raghavachari, A. Rendell, J. C. Burant, S. S. Iyengar, J. Tomasi, M. Cossi, N. Rega, J. M. Millam, M. Klene, J. E. Knox, J. B. Cross, V. Bakken, C. Adamo, J. Jaramillo, R. Gomperts, R. E. Stratmann, O. Yazyev, A. J. Austin, R. Cammi, C. Pomelli, J. W. Ochterski, R. L. Martin, K. Morokuma, V. G. Zakrzewski, G. A. Voth, P. Salvador, J. J. Dannenberg, S. Dapprich, A. D. Daniels, Ö. Farkas, J. B. Foresman, J. V. Ortiz, J. Cioslowski, and D. J. Fox, "Gaussian 09, revision d.01," Gaussian, Inc., Wallingford CT (2016).
- ³⁷A. D. Becke and R. M. Dickson, *J. Chem. Phys.* **89**, 2993 (1988).
- ³⁸A. Dreuw and M. Head-Gordon, *J. Am. Chem. Soc.* **126**, 4007 (2004).
- ³⁹A. D. Becke, *J. Chem. Phys.* **149**, 081102 (2018).